Research Article
Hittite Journal of Science and Engineering, 2023, 10 (3) 193–199
ISSN NUMBER: 2148–4171
DOI: 10.17350/HJSE19030000307

The Role of Rubrene Concentration on Dielectric Parameters of Nematic Liquid Crystal

Gulsum Kocakulah
Duzce University, Department of Physics, Duzce, Turkiye

ABSTRACT

In this study, the dielectric parameters of E7 coded nematic liquid crystal (NLC) composites containing the different amounts of rubrene fluorescent dye were investigated. E7, E7+0.5 wt.% Rubrene, and E7+1.0 wt.% Rubrene samples were prepared. Frequency dependent dielectric constants (ε′ and ε″), dielectric anisotropy (Δε′), and ac conductivity (σ_{ac}) graphs of rubrene doped E7 NLC composites were obtained by dielectric spectroscopy method and compared with pure E7 NLC. By using these graphs, relaxation frequency (f_R), relaxation time (τ_R), dielectric strength (δε′), and crossover frequency (f_c) parameters of the E7 NLC and its rubrene doped composites were determined. An increase in f_R from 3.045 MHz to 3.697 MHz for 0 V and from 627 kHz to 686 kHz for 40 V was observed with increasing rubrene concentration. On the other hand, a decrease in τ_R from 0.052 μs to 0.043 μs for 0 V and from 0.254 μs to 0.232 μs for 40 V was seen with increasing rubrene concentration. Furthermore, an increase in f_c from 1.145 MHz to 1.298 MHz was obtained with increasing rubrene concentration. The results show that the dielectric parameters change with the concentration of rubrene and it is thought that this study will provide a basis for investigating the dielectric properties of rubrene doped NLC composites. Moreover, it is concluded that the produced composites are a suitable base material for electro-optical device applications such as smart displays, photonics and electrical circuit elements.

Keywords:
Dielectric anisotropy; Nematic liquid crystal; Relaxation frequency; Relaxation time; Rubrene

Article History:
Received: 2022/12/29
Accepted: 2023/06/17
Online: 2023/09/30

***Correspondence to**: Gulsum Kocakulah,*
E-mail: gulsum.kocakulah@gmail.com,
Phone: +90 380 541 2404;
Fax: +90 380 541 2403

This article has been checked for similarity.

INTRODUCTION

Liquid crystals (LCs) are known as materials whose properties are between isotropic liquid and anisotropic crystal [1-3]. This fascinating feature of LCs has attracted the attention of many research groups for broad applications in various fields of science and technology. This materials widely used in smart windows [4, 5], displays [6, 7], sensors [8, 9], and other electro-optical device applications. Especially, nematic liquid crystal (NLC) is technologically considerable phases within LCs and it is broadly used in the field of display [10-12]. The molecular orientation of NLCs is quite responsive to external stimuli like electric and magnetic fields [13, 14]. In recent years, the physical properties of NLCs can be also developed with several dopant materials such as polymers [15, 16], dyes [17, 18], and nanoparticles [19-21]. These dopant materials affect the molecular orientation of NLCs and can change their physical properties. Although there are studies examining the electro-optical and dielectric properties of dye doped NLC composites in the literature, the number of studies investigating the dielectric properties of fluorescent dye doped NLCs is very few. Therefore, the use of fluorescent dye was preferred in order to observe the change in dielectric properties of E7 NLC in this research. Fluorescent dyes are defined as materials that both absorb and strongly emit in the visible region of the electromagnetic spectrum. Moreover, dyes with fluorescent properties are known as materials that distinguish from fluorescent brighteners that emit visible light but absorb ultraviolet [22]. The absorption characteristics of fluorescent dyes influence the orientation mechanisms of NLCs. Thus, the physical properties of LC based composites are significantly affected [23].

Rubrene, which is known as 5,6,11,12-tetraphenylnaphthacene, is composed of tetracene backbone and four phenyl groups substituted at the 5, 6, 11, 12 positions. Rubrene powder is red or light brown and has strong absorption in the blue-violet to green spectrum [24]. Moreover, this fluorescent dye is important due to

Cite as:
G. KOCAKULAH, "The Role of Rubrene Concentration on Dielectric Parameters of Nematic Liquid Crystal" Hittite Journal of Science and Engineering, 10(3): 193–199, 2023. doi:10.17350/hjse19030000307

emission properties, electrical conductivity and mobility [25]. It is a p-type organic semiconductor with an emission wavelength of 550 nm [24, 26]. In addition, the carrier mobility in organic field effect transistors is quite high [27, 28]. Rubrene, which has unique physical and chemical properties, has been used in many electro-optical device applications such as field-effect transistors [29], organic light-emitting diodes [30], and solar cells [31, 32] until today.

This paper reports the effect of rubrene concentration on the dielectric parameters of E7 NLC. The frequency dependent dielectric parameters (dielectric constants: ε′ and ε″, dielectric anisotropy: Δε′, and ac conductivity: σ_{ac}) of pure and rubrene doped samples were investigated for Planar-state (V=0 V) and Homeotropic-state (V=40 V). In addition, relaxation frequency (f_R), crossover frequency (f_C), relaxation time (τ_R), and dielectric strength (δε′) parameters of the samples were obtained using these data. The results showed that rubrene caused a significant change in dielectric parameters of E7 NLC.

MATERIAL AND METHODS

The E7 NLC (n_o=1.521 and n_e=1.746) used in the experiment was purchased from Instec. This material consists of 4-cyano-4′-n-pentyl-biphenyl (5CB, 51 wt.%), 4-cyano-4′-n-heptyl-biphenyl (7CB, 25 wt.%), 4-cyano-4′-n-octyloxy-biphenyl (80CB, 16 wt.%), and 4-cyano-4″-n-pentyl-p-terphenyl (5CT, 8 wt.%). The phase transition temperature of E7 NLC nematic phase to isotropic phase (T_{N-I}) is 60.5 °C. Rubrene fluorescent dye (sublimed grade and λ_{em}=550 nm) was provided from Sigma Aldrich. The molecular formulas of the E7 and rubrene were given in Figure 1(a-b). Also, indium thin oxide (ITO) coated planar aligned LC cells has been used for the measurements and purchased from Instec. The 18 μm spacer was used in the cells, and the surface resistance of the ITO coated glass plates was given as a 25 Ω/cm².

Schematic representation of the sample preparations and measurements procedure was given in Figure 2(a-d). Firstly, rubrene doped NLC composites were prepared with a concentration of 0.5 wt.% and 1.0 wt.% (Figure 2(a)). Then, composites was homogenised in an ultrasonic bath for 5 hour at 80 °C (Figure 2(b)). Finally, pure E7 NLC and rubrene doped E7 NLC composites were filled into the LC cells with the above specifications by capillary method (Figure 2(c)). Produced samples were coded as: E7, E7+0.5 wt.% Rubrene, and E7+1.0 wt.% Rubrene.

Dielectric parameters of pure and rubrene doped E7 NLC was determined with a computer-controlled Novocontrol Alpha-A Dielectric/Impedance Analyzer between 1 kHz and 10 MHz with a test signal of 100 mV_{rms} for 0 V and 40 V at room temperature (Figure 2(d)).

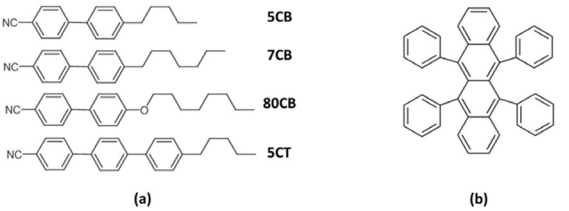

Figure 1. The molecular formula of the (a) E7 NLC and (b) Rubrene fluorescent dye.

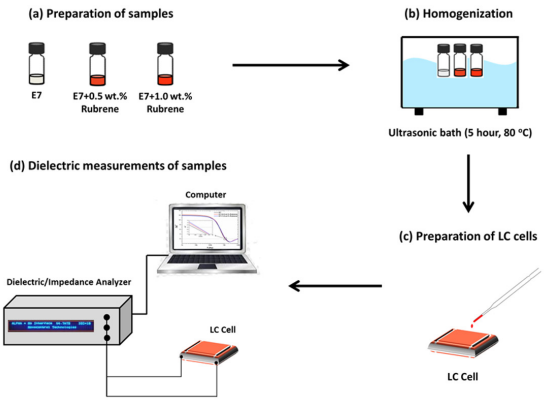

Figure 2. Schematic representation of the sample preparations and measurements.

RESULTS AND DISCUSSION

Dielectric response of LC materials show complex behaviour and provides information about molecular polarizability and dipole moment when an electric field is applied. The complex dielectric constant acts as the most considerable parameter in determining the dielectric behaviour of LCs and is given by the following formula [33, 34]:

$$\varepsilon^* = \varepsilon' - i\varepsilon'' \tag{1}$$

where, ε′ and ε″ is real and imaginary parts of the complex dielectric constant, respectively. Also, ε′ is energy stored in materials and defines as [35]:

$$\varepsilon' = \frac{Cd}{\varepsilon_o A} = \frac{C}{C_o} \tag{2}$$

where, C is the capacitance and C_o is the capacitance of the free space. Also, d is the thickness and A is the area of the LC cell. ε_o is dielectric constant of free space. Besides, ε″ denotes loss of energy in materials and defines as [35]:

$$\varepsilon'' = \frac{Gd}{\omega\varepsilon_o A} = \frac{G}{\omega C_o} \tag{3}$$

where, ω is the angular frequency and G is the conductance.

Figure 3(a-b) demonstrates the frequency dependent ε′ comparison graphs of the samples for 0 V and 40 V. Small changes occurred in ε′ value for both 0 V and 40 V depending on the increasing rubrene concentration. These small increases and decreases were seen in the low frequency regions. The reasons for these changes will be given in the explanations of Figure 4(a-b). Furthermore, in order to observe the voltage dependent ε′ values of the pure E7 NLC and rubrene doped E7 NLC composites, the frequency dependent ε′ variation graphs were given in Figure 3(c-e) for each sample. As seen in the figures, the ε′ parameters of all samples increased due to the increase in voltage. This increment can be clarified by the regular orientation of both LC and rubrene molecules in the electric field direction with changing voltage. Moreover, it is seen that the ε′ parameters of the samples at 0 V are almost the same 1 kHz-1 MHz frequency range, but decrease rapidly after 1 MHz. Therewithal, for 40 V, it is also observed that the ε′ parameter does not almost change in the 1 kHz-100 kHz frequency range for all samples and reduces after 100 kHz. The results show that samples will show relaxation after these frequency values.

The ε′-f comparison graphs of the samples at 1 kHz-10 kHz frequency range that changes depending on the rubrene concentration were given in Figure 4(a-b). The ε′ increased for E7+0.5 wt.% Rubrene while it decreased for E7+1.0 wt.% Rubrene. Some interactions are thought to occur in the composites when E7 NLC doped with rubrene: NLC-NLC, rubrene-rubrene and NLC-rubrene. The interactions between E7 NLC and rubrene dye molecules can be dipolar, electrostatic, and van der Waals. In this study, ε′ value increases in the low frequency region given in the graph for E7+0.5 wt.% Rubrene compared to pure E7 NLC for 0 V and 40 V. The reason for this behaviour is the increased dipole moment due to molecular interactions between NLC and rubrene. On the other hand, the number of domains in the composites decreases with increasing rubrene concentration. Thus, the distance between the domains increases and the dipole-dipole interactions decrease. For this reason, ε′ low for E7+1.0 wt.% Rubrene than for E7+0.5 wt.% Rubrene [36].

In Figure 5(a-b), the frequency dependent ε″ comparison graphs of the samples were given for 0 V and 40 V. Similar to the ε′ parameter, it is seen that small changes occur in ε″ values depending on the increasing rubrene concentration. In addition, it was desired to examine the ε″ variation graphs of the samples depending on both voltage and frequency, separately for each sample. For this reason, graphs of the variation of ε″ parameter with voltage were given in

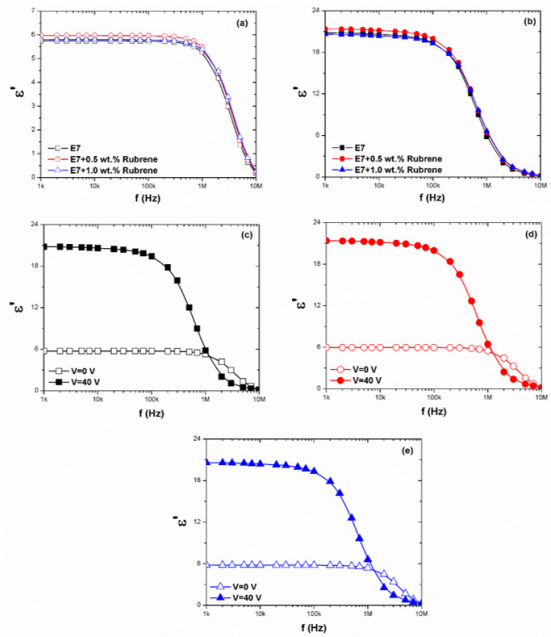

Figure 3. ε′-f comparison graphs of the samples (a) V=0 V and (b) V=40 V. Also, ε′-f single graphs of (c) E7, (d) E7+0.5 wt.% Rubrene, and (e) E7+1.0 wt.% Rubrene.

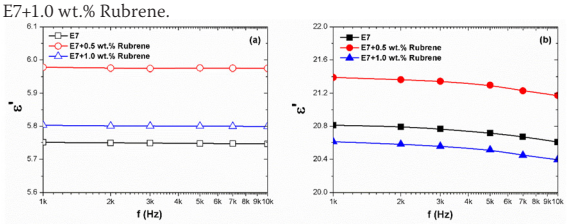

Figure 4. ε′-f comparison graphs of the samples at 1 kHz -10 kHz frequency range for (a) 0 V and (b) 40 V.

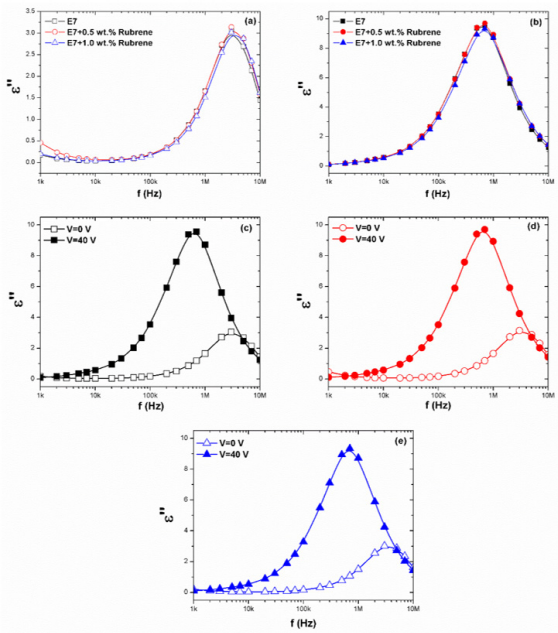

Figure 5. ε″-f comparison graphs of the samples (a) V=0 V and (b) V=40 V. Also, ε″-f single graphs of (c) E7, (d) E7+0.5 wt.% Rubrene, and (e) E7+1.0 wt.% Rubrene.

Figure 5(c-e) for pure E7 NLC and rubrene doped E7 NLC composites. It is seen that the ε'' values increase in all samples depending on the regular molecular arrangement with increasing voltage. Additionally, a single peak was observed between 1 kHz and 10 MHz for E7 NLC and its rubrene doped composites. This behaviour indicates that the samples have a single relaxation frequency in the examined frequency range. The relaxation frequency (f_R) of the samples is determined using the frequencies corresponding to the peak points of the ε''-f graphs. The f_R values of E7 NLC and rubrene doped E7 NLC composites were given in Table 1. From the table, it is seen that the f_R increases with increasing rubrene concentration for 0 V and 40 V. The increase in f_R values of rubrene doped E7 NLC composites compared to pure E7 NLC may be owing to the increased availability of free space for molecular motion due to the presence of rubrene. Also, it is thought that the reduction in rotational viscosity with the addition of rubrene is also effective in the increase of f_R [37].

Table 1. Relaxation frequency (f_R), relaxation time (τ_R), and dielectric strength (δε′) parameters of the E7, E7+0.5 wt.% Rubrene, and E7+1.0 wt.% Rubrene for 0 V and 40 V.

	V=0 V			V=40 V		
	f_R (MHz)	τ_R (μs)	δε'	f_R (kHz)	τ_R (μs)	δε'
E7	3.045	0.052	5.581	627	0.254	20.679
E7+0.5 wt.% Rubrene	3.322	0.048	5.773	657	0.242	21.201
E7+1.0 wt.% Rubrene	3.697	0.043	5.541	686	0.232	20.409

The complex dielectric constant is also defined with Cole-Cole equation [38, 39]:

$$\varepsilon^* = \varepsilon_\infty^{'} + \frac{\varepsilon_s^{'} - \varepsilon_\infty^{'}}{1+\left(i\omega\tau_R\right)^{1-\alpha}} \quad (4)$$

where, ε'_s is the low and ε'_∞ is the high frequency limit of the ε′, τ_R is relaxation time and α is relaxation distribution parameter. If α=0, the Cole-Cole model called as Debye model. In this case, the system has a single relaxation time. And if α≠0, the relaxation behaviour fits non-Debye model and system has a more than one relaxation processes [40, 41].

Figure 6(a-b) indicates the Cole-Cole comparison graphs of E7 NLC and rubrene doped E7 NLC composites for 0 V and 40 V. Moreover, Cole-Cole graphs obtained at 0 V and 40 V for each sample were given in Figure 6(c-e). It has been observed that the samples almost complete the semicircle and behave according to the Debye model. The τ_R of E7 NLC and rubrene doped E7 NLCs were calculated using the Cole-Cole plots and their values were given in Table 1. It is observed that the τ_R increases in both E7 NLC and rubrene doped E7 NLC composites depending on the increasing voltage. The cause for this attitude is that the molecular orientation increases with increasing voltage, thus increasing the time it takes for LC and rubrene to return to their initial state. Besides, it is seen that τ_R reduces with increasing rubrene concentration in E7 NLC for 0 V and 40 V. This behaviour can be explained by the fact that the trapping of free ions in the rubrene doped composites. As a result of the decrease in ion concentration, the viscosity of the composites decreases, thus the relaxation time of the system is also reduced [42]. This result is important in that E7 NLC doped with rubrene shows relaxation behaviour in a shorter time.

Dielectric strength (δε′) is determined using the Cole-Cole graphs of the samples and calculated by the following equation [37, 41]:

$$\delta\varepsilon' = \varepsilon_s^{'} - \varepsilon_\infty^{'} \quad (5)$$

The δε′ values of the samples were given in Table 1. According to table, δε′ of pure E7 NLC and rubrene doped E7 NLC composites increase depending on the voltage. The main reason for this increase is that ε'_s increases with increasing voltage. According to the change in rubrene concentration, there is a small increase in E7+0.5 wt.% Rubrene and a small decrease in E7+1.0 wt.% Rubrene when compared with the δε′ value of E7 NLC. The results indicate that rubrene concentration causes a change in the δε′.

Dielectric anisotropy (Δε′) is the significant parameter for LC-based electro-optical devices and defined as the difference between parallel ($\varepsilon'_{\parallel}$) and perpendicular ($\varepsilon'_{\perp}$) components of the ε' values [23, 38]:

$$\Delta\varepsilon^{'} = \varepsilon_{\parallel}^{'} - \varepsilon_{\perp}^{'} \quad (6)$$

In Figure 7, the frequency dependent Δε′ change graph of the samples was given. It is seen from the graph that the Δε′ value of E7+0.5 wt.% Rubrene increases slightly compared to E7 NLC at 1 kHz-100 kHz frequency range. In E7+1.0 wt.% Rubrene, it is observed that there is a small decrease in Δε′ compared to E7 NLC in the same frequency range. In addition, the crossover frequency (f_C) of the samples is determined using the Δε′-f graph. The f_C values of E7, E7+0.5 wt.% Rubrene, and E7+1.0 wt.% Rubrene were determined in the 1 MHz-2 MHz frequency range where the Δε′-f graph changed from positive to negative. Using the data inset of the graph, the fc values of E7, E7+0.5 wt.% Rubrene, and E7+1.0 wt.% Rubrene were calculated as 1.145 MHz, 1.250

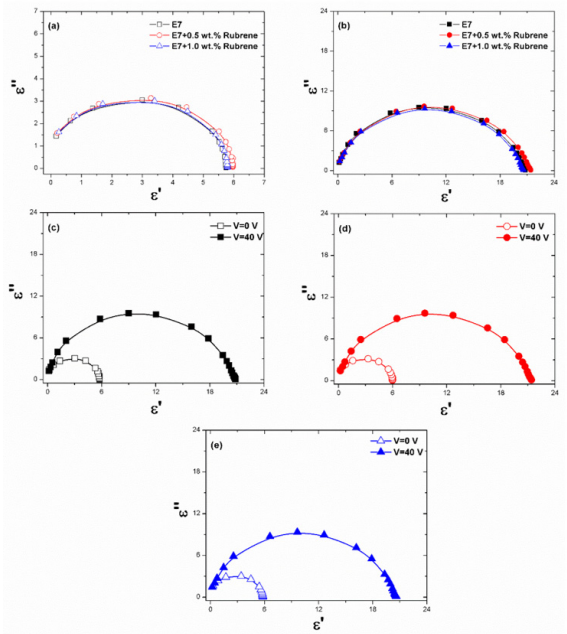

Figure 6. Cole-Cole comparison graphs of the samples (a) V=0 V and (b) V=40 V. Also, Cole-Cole single graphs of (c) E7, (d) E7+0.5 wt.% Rubrene, and (e) E7+1.0 wt.% Rubrene.

MHz and 1.298 MHz, respectively. According to the data, it can be seen that the f_C values of the rubrene doped E7 NLCs increased when compared to E7 NLC. In rubrene doped E7 NLCs, the interactions between rubrene and NLC molecules cause some changes in the molecular structure of the composite. Furthermore, these interactions change with increasing rubrene concentration. Depending on these changes, the interaction of the molecules with the longitudinal and transverse dipole moments in the electric field changes with frequency. Accordingly, it is thought that the increase in the f_C values of the rubrene doped composites is related to the change in the phase structure.

The ac conductivity of materials is given by the following equation [43, 44]:

$$\sigma_{ac} = \varepsilon_o \omega \varepsilon'' \quad (7)$$

Figure 8(a-b) depicts that frequency dependent σ_{ac} comparison graphs of the E7 NLC and its rubrene doped composites for 0 V and 40 V. The small increases and decreases in the σ_{ac} parameter of the samples with increasing rubrene concentration cannot be clearly seen from the graphs. However, it is seen that the σ_{ac} values of both E7 NLC and rubrene doped E7 NLC composites increase with increasing frequency for 0 V and 40 V. For a more detailed analysis, σ_{ac}-f graphs for each sample were given in Figure 8(c-e). The σ_{ac} values increased with increasing voltage. Moreover, in Figure 8(f), σ_{ac} value of the samples at 1 kHz was given. As seen in the graph, there is a minor increment in the σ_{ac} of the

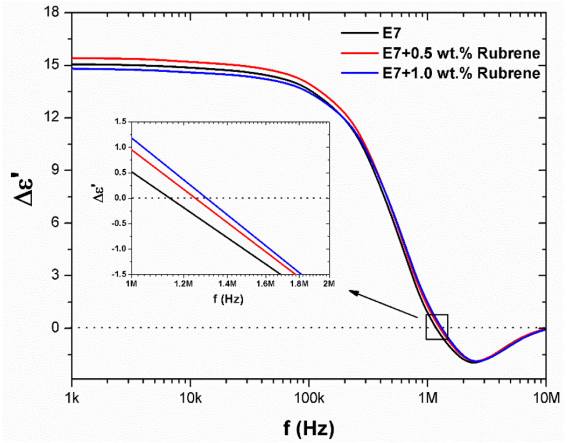

Figure 7. Δε'-f graph of the E7, E7+0.5 wt.% Rubrene, and E7+1.0 wt.% Rubrene.

E7+0.5 wt.% Rubrene compared to the E7 NLC. This behaviour can be explained by the mobility of NLC and rubrene molecules. However, it is observed that the σ_{ac} value of the E7+1.0 wt.% Rubrene is quite close to the E7 NLC and is less than E7+0.5 wt.% Rubrene. This reduction may be related to the restriction caused by feeble aggregations in E7+1.0 wt.% Rubrene [11].

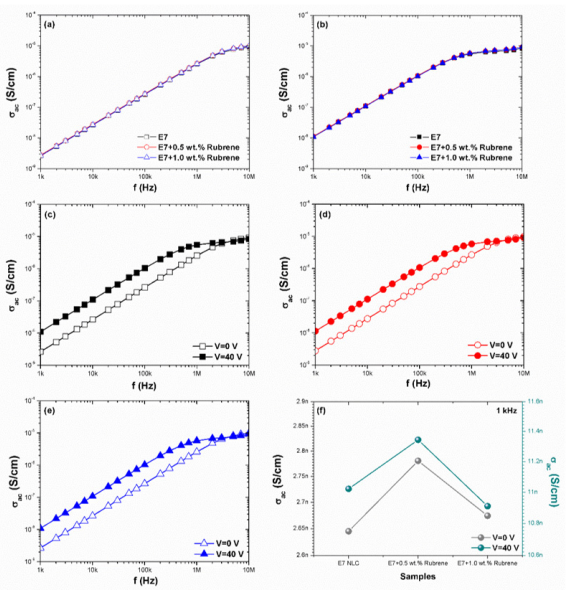

Figure 8. σ_{ac}-f comparison graphs of the samples (a) V=0 V and (b) V=40 V. Also, σ_{ac}-f single graphs of (c) E7, (d) E7+0.5 wt.% Rubrene, and (e) E7+1.0 wt.% Rubrene. And (f) σ_{ac} value of the samples at 1 kHz.

CONCLUSION

In the current study, the dielectric parameters of rubrene doped E7 NLC were investigated. In order to observe the rubrene effect, two different concentrations were used and the dielectric parameters of the produced E7+0.5 wt.% Rubrene and E7+1.0 wt.% Rubrene composites were

compared with the pure E7 NLC. Dielectric measurements were carried out at 0 V and 40 V, depending on the frequency. As a result of the experimental evaluations, it was concluded that f_R increases and τ_R decreases with increasing rubrene concentration in E7 NLC. In addition, it was observed that the frequency dependent $\Delta\varepsilon'$ of the samples were quite close to each other and f_C was calculated from the $\Delta\varepsilon'$-f graphs. It was found that the f_C increased with rubrene concentration in E7 NLC. Accordingly, rubrene doped E7 NLCs will be considerable for the production of electro-optical devices with low relaxation time that can operate in the high frequency region.

CONFLICT OF INTEREST

The authors declare that they have no known competing financial interests or personal relationships that could have appeared to influence the work reported in this paper.

REFERENCES

1. Varshney D, Anu, Prakash J, Singh VP, Yadav K, Singh G. Probing the Impact of Bismuth-titanate Based Nanocomposite on the Dielectric and Electro-Optical Features of a Nematic Liquid Crystal Material. Journal of Molecular Liquids. 2022;347:118389.
2. Mani S, Patwardhan S, Hadkar S, Mishra K, Sarawade P. Effect of Polymer Concentration on Optical and Electrical Properties of Liquid Crystals for Photonic Applications. Materials Today: Proceedings. 2022;62:7035-7039.
3. Mishra R, Hazarika J, Hazarika A, Gogoi B, Dubey R, Bhattacharjee D, Singh KN, Alapati PR. Dielectric Properties of a Strongly Polar Nematic Liquid Crystal Compound Doped with Gold Nanoparticles. Liquid Crystals. 2018;45(11):1661-1671.
4. Oh SW, Ji SM, Han CH, Yoon TH. A Cholesteric Liquid Crystal Smart Window with a Low Operating Voltage. Dyes and Pigments. 2022;197:109843.
5. Jinqian L, Zhao Y, Gao H, Wang D, Miao Z, Cao H, Yang Z, He W. Polymer Dispersed Liquid Crystals Doped with CeO2 Nanoparticles for the Smart Window. Liquid Crystals. 2022;49(1):29-38.
6. Li YL, Li NN, Wang D, Chu F, Lee SD, Zheng YW, Wang QH. Tunable Liquid Crystal Grating Based Holographic 3D Display System with Wide Viewing Angle and Large Size. Light: Science & Applications. 2022;11:188.
7. Tan G, Huang Y, Li MC, Lee SL, Wu ST. High Dynamic Range Liquid Crystal Displays with a Mini-LED Backlight. Optics Express. 2018;26(13):16572-16584.
8. Mulder DJ, Schenning APHJ, Bastiaansen CWM. Chiral-Nematic Liquid Crystals as One Dimensional Photonic Materials in Optical Sensors. Journal of Materials Chemistry C. 2014;2:6695-6705.
9. Cachelin P, Green JP, Peijs T, Heeney M, Bastiaansen CWM. Optical Acetone Vapor Sensors Based on Chiral Nematic Liquid Crystals and Reactive Chiral Dopants. Advanced Optical Materials. 2016;4(4):92-596.
10. Pathak G, Hegde G, Prasad V. Investigation of Electro-Optical and Dielectric Properties of Nematic Liquid Crystal Dispersed with Biowaste Based Porous Carbon Nanoparticles: Increased Birefringence for Display Applications. Journal of Molecular Liquids. 2020; 314:113643.
11. Yadav G, Kumar M, Srivastava A, Manohar R. SiO2 Nanoparticles Doped Nematic Liquid Crystal System: An Experimental Investigation on Optical and Dielectric Properties. Chinese Journal of Physics. 2019;57:82-89.
12. Özğan Ş, Eskalen H, Tapkıranlı Y. The Electrical and Optical Behavior of Graphene Oxide Doped Nematic Liquid Crystal. Journal of Materials Science: Materials in Electronics. 2022;33:5720-5729.
13. Yadav G, Agrahari K, Manohar R. Multiwall Carbon Nanotube-Nematic Liquid Crystal Composite System: Preparation and Characterization. Journal of Dispersion Science and Technology. 2021;42(5):707-714.
14. Varshney D, Parveen A, Prakash J. Effect of Cobalt Oxide Nanoparticles on Dielectric Properties of a Nematic Liquid Crystal Material. Journal of Dispersion Science and Technology. 2022;43(1):42-49.
15. Pandey S, Gupta SK, Singh DP, Vimal T, Tripathi PK, Srivastava A, Manohar R. Effects of Polymer Doping on Dielectric and Electro-Optical Parameters of Nematic Liquid Crystal. Polymer Engineering & Science. 2015;55(2):414-420.
16. Kim Y, Jung D, Jeong S, Kim K, Choi W, Seo Y. Optical Properties and Optimized Conditions for Polymer Dispersed Liquid Crystal Containing UV Curable Polymer and Nematic Liquid Crystal. Current Applied Physics. 2015;15(3):292-297.
17. Eskalen H, Özğan Ş, Okumuş M, Kerl S. Thermal and Electro-Optical Properties of Graphene Oxide/Dye-Doped Nematic Liquid Crystal. Brazilian Journal of Physics. 2019;49: 341-347.
18. Ye L, Hou C, Lv C, Zhao C, Yin Z, Cui Y, Lu Y. Tailoring of Random Lasing Characteristics in Dye-Doped Nematic Liquid Crystals. Applied Physics B. 2014;115:303-309.
19. Chemingui M, Singh UB, Yadav N, Dabrowski RS, Dhar R. Effect of Iron Oxide (γ-Fe2O3) Nanoparticles on the Morphological, Electro-Optical and Dielectric Properties of a Nematic Liquid Crystalline Material. Journal of Molecular Liquids. 2020;319:114299.
20. Praseetha KP, Shiju E, Chandrasekharan K, Varghese S. Intense Nonlinear Optical Properties of ZnS Quantum Dot Doped Nematic Liquid Crystal Compounds. Journal of Molecular Liquids. 2021;328:115347.
21. Elkhalgi HHM, Khandka S, Singh UB, Pandey KL, Dabrowski R, Dhar R. Dielectric and Electro-Optical Properties of a Nematic Liquid Crystalline Material with Gold Nanoparticles. Liquid Crystals. 2018;45(12):1795-1801.
22. Christie RM. Handbook of Textile and Industrial Dyeing Principles, Processes and Types of Dyes. Volume 1 in Woodhead Publishing Series in Textiles; 2011. p. 562-587.
23. Pathak G, Agrahari K, Yadav G, Srivastava A, Strzezysz O, Manohar R. Tuning of Birefringence, Response Time, and Dielectric Anisotropy by the Dispersion of Fluorescent Dye into the Nematic Liquid Crystal. Applied Physics A. 2018;124:463.
24. Liu S, Wu H, Zhang X, Hu W. Research Progress of Rubrene as an Excellent Multifunctional Organic Semiconductor. Frontiers of Physics. 2021;16(1):13304.
25. Al-Muntaser AA, Alamri HR, Sharma K, Eltahir S, Makhlouf MM. Role of Rubrene Additive for Reinforcing the Structural, Optical, and Dispersion Properties of Polyvinyl Alcohol Films Towards Optoelectronic Applications. Optical Materials. 2022;128:112465.
26. Selvaraj P, Li P-Y, Antony M, Wang Y-W, Chou P-W, Chen Z-H, Hsu C-J, Huang C-Y. Rubbing-Free Liquid Crystal Electro-Optic Device Based on Organic Single-Crystal Rubrene. Optics Express. 2022;30(6):9521-9533.
27. Ma H, Liu N, Huang J-D. A DFT Study on the Electronic Structures and Conducting Properties of Rubrene and Its Derivatives in Organic Field-Effect Transistors. Scientific Reports. 2017;7:331.

28. Podzorov V, Menard E, Rogers JA, Gershenson ME. Hall Effect in the Accumulation Layers on the Surface of Organic Semiconductors. Physical Review Letters. 2005;95(22): 226601.
29. Kim K, Kim MK, Kang HS, Cho MY, Joo J, Kim JH, Kim KH, Hong CS, Choi DH. New Growth Method of Rubrene Single Crystal for Organic Field-Effect Transistor. Synthetic Metals. 2007;157(10-12):481-484.
30. Wang X, Wang R, Zhou D, Yu J. Study of Organic Light-Emitting Diodes with Exciplex and Non-Exciplex Forming Interfaces Consisting of an Ultrathin Rubrene Layer. Synthetic Metals. 2016;214:50-55.
31. Pelicano CM, Yanagi H. Effect of Rubrene:P3HT Bilayer on Photovoltaic Performance of Perovskite Solar Cells with Electrodeposited ZnO Nanorods. Journal of Energy Chemistry. 2018;27(2):455-462.
32. Huang J, Yu J, Wang W, Jiang Y. Organic Solar Cells with a Multicharge Separation Structure Consisting of a Thin Rubrene Fluorescent Dye for Open Circuit Voltage Enhancement. Applied Physics Letters. 2011;98:023301.
33. Nasri R, Missaoui T, Hbibi A, Soltani T. Enhanced Dielectric Properties of Nematic Liquid Crystal Doped with Ferroelectric Nanoparticles. Liquid Crystals. 2021;48(10):1429-1437.
34. Jain AK, Deshmukh RR. Effects of Dye Doping on Electro-Optical, Thermo-Electro-Optical and Dielectric Properties of Polymer Dispersed Liquid Crystal Films. Journal of Physics and Chemistry of Solids. 2022;160:110363.
35. Tüzün Özmen Ö, Goksen K, Demir A, Durmus M, Köysal O. Investigation of Photoinduced Change of Dielectric and Electrical Properties of Indium (III) Phthalocyanine and Fullerene Doped Nematic Liquid Crystal. Synthetic Metals. 2012;162(24):2188-2192.
36. Pathak G, Agrahari K, Roy A, Srivastava A, Strzezysz O, Garbat K, Manohar R. Dispersion of Fluorescent Dye in the Nematic Liquid Crystal: Enhanced Photoluminescence and High Birefringence. Opto-Electronics Review. 2018;26:317-324.
37. Mishra S, Sontakke AM, Gupta RK, Kumar S, Manjuladevi V. Dielectric Spectroscopy Studies of Silver Nanorod Doped Nematic Liquid Crystal. Materials Today: Proceedings. 2022;50:2587-2591.
38. Manohar R, Pandey KK, Srivastava AK, Misra AK, Yadav SP. Sign Inversion of Dielectric Anisotropy in Nematic Liquid Crystal by Dye Doping. Journal of Physics and Chemistry of Solids. 2010;71:1311-1315.
39. Pandey KK, Bawaria AK, Priyadarshi P. Effect of Nano Particles on the Dielectric Anisotropy of Liquid Crystal. Journal of Scientific Research and Advances. 2015;2(3):103-107.
40. Deshmukh RR, Jain AK. The Complete Morphological, Electro-Optical and Dielectric Study of Dichroic Dye-Doped Polymer-Dispersed Liquid Crystal. Liquid Crystals. 2014; 41(7):960-975.
41. Deshmukh RR, Jain AK. Effect of Anti-Parallel and Twisted Alignment Techniques on Various Properties of Polymer Stabilised Liquid Crystal (PSLC) Films. Liquid Crystals. 2016;43(4):436-447.
42. Salah MB, Nasri R, Alharbi AN, Althagafi TM, Soltani T. Thermotropic Liquid Crystal Doped with Ferroelectric Nanoparticles: Electrical Behavior and Ion Trapping Phenomenon. Journal of Molecular Liquids. 2022;357:119142.
43. Jayoti D, Khushboo, Malik P, Singh A. Effect of Polymer Concentration on Morphology, Dielectric and Optical Properties in a Polymer-Dispersed Ferroelectric Liquid Crystal. Liquid Crystals. 2016;43(5):623-631.
44. Vimal T, Agrahari K, Sonker RK, Manohar R. Investigation of Thermodynamical, Dielectric and Electro-Optical Parameters of Nematic Liquid Crystal Doped with Polyaniline and Silver Nanoparticles. Journal of Molecular Liquids. 2019;290:111241.